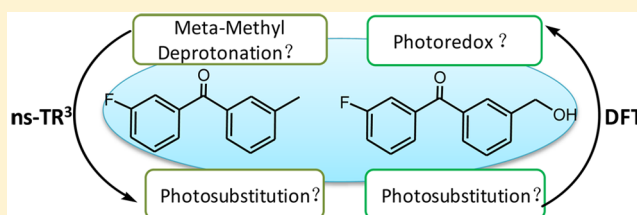


# Competition between “Meta Effect” Photochemical Reactions of Selected Benzophenone Compounds Having Two Different Substituents at Meta Positions

Jiani Ma,<sup>\*,†</sup> Huai Li,<sup>†</sup> Xiting Zhang,<sup>‡</sup> Wen-Jian Tang,<sup>§</sup> Mingde Li,<sup>‡</sup> and David Lee Phillips<sup>\*,‡</sup><sup>†</sup>Key Laboratory of Synthetic and Natural Functional Molecule Chemistry of Ministry of Education, College of Chemistry and Materials Science, Northwest University, 229 Taibai N Road, Xi'an, Shaanxi, People's Republic of China<sup>‡</sup>Department of Chemistry, The University of Hong Kong, Pokfulam Road, Hong Kong 11111<sup>§</sup>School of Pharmacy, Anhui Medical University, Meishan Road 81, Hefei 230032, People's Republic of China

## Supporting Information

**ABSTRACT:** Recent studies conducted on some “meta effect” photochemical reactions focused on aromatic carbonyls having a substitution on one meta position of the benzophenone (BP) and anthraquinone parent compound. In this paper, two different substitutions were introduced with one at each meta position of the BP parent compound to investigate possible competition between different types of meta effect photochemistry observed in acidic solutions containing water. The photochemical pathways of 3-hydroxymethyl-3'-fluorobenzophenone (1) and 3-fluoro-3'-methylbenzophenone (2) were explored in several solvents, including acidic water-containing solutions, using time-resolved spectroscopic experiments and density functional theory computations. It is observed that 1 can undergo a photoredox reaction and 2 can undergo a meta-methyl deprotonation reaction in acidic water-containing solutions. Comparison of these results to those previously reported for the analogous BP derivatives that contain only one substituent at a meta position indicates the introduction of electron-donating (such as hydroxyl) and electron-withdrawing groups (such as F) on the meta positions of BP can influence the meta effect photochemical reactions. It was found that involvement of an electron-donating moiety facilitates the meta effect photochemical reactions by stabilizing the crucial reactive biradical intermediate associated with the meta effect photochemical reactions.



## INTRODUCTION

Proton transfer reactions can be found in many chemistry and biology processes.<sup>1</sup> The carbonyl oxygen protonation in aromatic carbonyl molecules in their excited states in acidic water-containing solutions is of great interest from a range of different aspects in photochemistry.<sup>2</sup> Wirz and co-workers examined the protonation of the carbonyl oxygen of the excited state of several benzophenone (BP) compounds and saw that an acid-catalyzed photohydration reaction can occur in acidic aqueous solutions.<sup>3</sup> It was suggested that the protonated triplet state species could cause noticeable delocalization at the meta and ortho points of the benzene group. This is consistent with activation of the meta and ortho sites in the benzyl group and Zimmerman's ortho–meta effect in photochemical reactions.<sup>4</sup> Several research groups, such as Scaiano and co-workers and Miranda and co-workers, have done systematic studies on the photophysical and photochemical pathways resulting from the protonation of carbonyl compounds using steady-state spectroscopy methods and laser flash photolysis.<sup>5,6</sup> Wan and co-workers contributed in this research area with the investigation of novel and efficient photoredox reactions resulting from the protonation of aromatic carbonyl compounds, such as BP and anthraquinone (AQ) derivatives. It was shown that the ketone

can be reduced to an alcohol while accompanied by a side chain alcohol being oxidized to its ketone for a BP or AQ derivative containing an alcohol side chain attached to a meta position of a phenyl ring.<sup>7</sup> As these photochemical reactions were not detected for the para counterpart BP compounds under analogous experimental conditions, these new photochemical reactions were described as “meta effect” photochemical reactions.<sup>7</sup> The photochemistry of other meta-substituted benzophenone derivatives like ketoprofen (KP) are also of interest because irradiation of KP is known to induce phototoxicity that limits its use in drug applications.<sup>5e,f</sup> KP-based derivatives have also been developed for use as photoremovable protecting groups that have potential applications for organic synthesis, drug delivery, and photo-triggers that can release biological effectors very fast and efficiently for use in biological experiments.<sup>6d–f</sup> An improved understanding of the photochemistry of a variety of meta-substituted BP compounds in water-containing media of varying pH may be of use in developing KP and other kinds

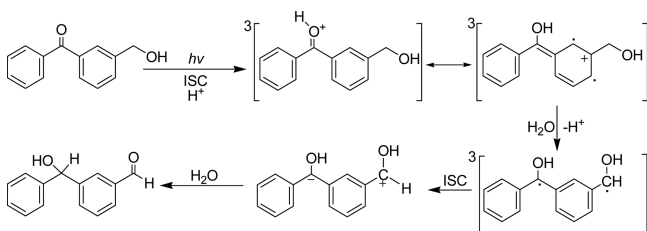
Received: April 1, 2016

Published: September 23, 2016

of *meta*-substituted benzophenone compounds as photo-protecting groups for a range of applications in the future.

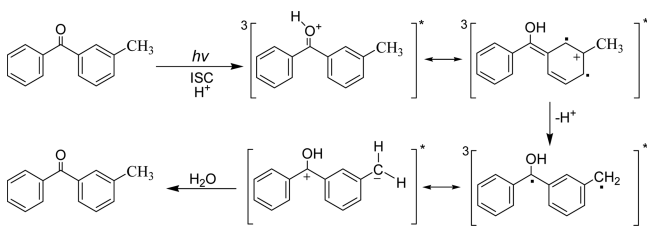
We have investigated the photochemical reaction mechanisms associated with the protonation of aromatic carbonyl molecules in recent years with time-resolved spectroscopic methods and DFT calculations.<sup>8</sup> Time-resolved resonance Raman (TR<sup>3</sup>) spectroscopy can provide a useful fingerprint for transient reactive intermediates to be particularly useful in more clearly determining the structure, character, and identity of the excited states and intermediates associated with the photochemical reactions explored.<sup>8</sup> Previously, a time-resolved spectroscopic investigation was done for 3-(hydroxymethyl)-benzophenone (*m*-BPOH) that directly characterized the transient species and observed a biradical intermediate that was associated with the photoredox reaction of interest (see Scheme 1).<sup>8b</sup> Evidence was also found that a *meta*-methyl

**Scheme 1. Reaction Mechanism Proposed for the Photoredox of *m*-BPOH<sup>8b</sup>**



deprotonation reaction can occur after photolysis of 3-methylbenzophenone (3-MeBP) in acidic water-containing solutions based on results from mass spectroscopy, and the proposed reaction mechanism is given in Scheme 2.<sup>7b,8d</sup>

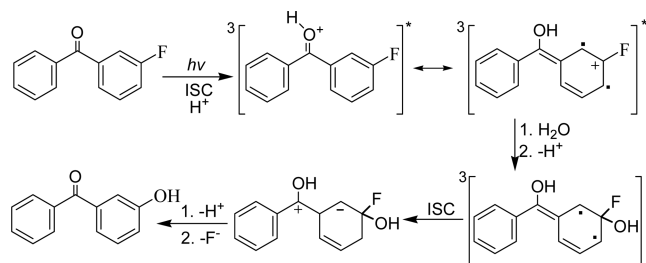
**Scheme 2. Reaction Mechanism Proposed for the *meta*-Methyl Deprotonation Reaction of 3-MeBP<sup>8d</sup>**



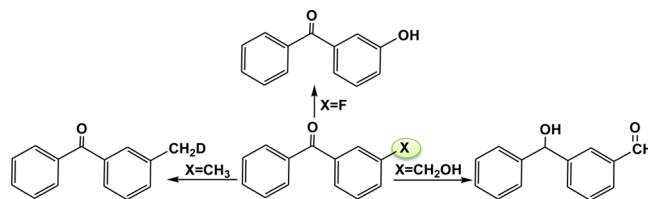
Photolysis of 3-MeBP in acidic D<sub>2</sub>O (CH<sub>3</sub>CN cosolvent) (pD < 3) resulted in introduction of deuterium to the *meta*-methyl group.<sup>7</sup> Wirz and co-workers reported that 3-fluorobenzophenone (3-FBP) may undergo an unusual and efficient photosubstitution reaction to yield 3-hydroxybenzophenone.<sup>3</sup> We recently performed some time-resolved spectroscopy experiments and theoretical computations to gain some insight into how the photosubstitution occurs for 3-FBP (see Scheme 3).<sup>8e</sup> The overall photoredox, *meta*-methyl deprotonation, and photosubstitution reactions, respectively, for *m*-BPOH, 3-MeBP, and 3-FBP are depicted in Scheme 4.

Previous studies conducted on *meta* effect photochemical reactions focused on aromatic carbonyls having a substitution on one of the *meta* positions of the BP and AQ parent compounds. It is not clear how the BP compounds will behave when two *meta* positions are substituted by two different groups in which there may be competition among the photoredox, photosubstitution, or *meta*-methyl deprotonation

**Scheme 3. Reaction Mechanism Proposed for the Photosubstitution of 3-FBP<sup>8e</sup>**



**Scheme 4. Some of the Novel *Meta* Effect Photochemical Reactions of BP Compounds Having Different Substituents on the *Meta* Position in Acidic Aqueous Solutions<sup>8b,d,e</sup>**



reactions. For example, when F and hydroxymethyl appear on each of the *meta* positions of the BP molecule, such as in 3-hydroxymethyl-3'-fluorobenzophenone (**1**), we do not know which photochemical reaction will take place and to what extent for the possible photosubstitution, photoredox, or photohydration reactions or even if some other novel photochemical reaction will occur. Here, we take **1** and 3-fluoro-3'-methylbenzophenone (**2**) (see the chemical structures in Figure 1) as example compounds to explore the above

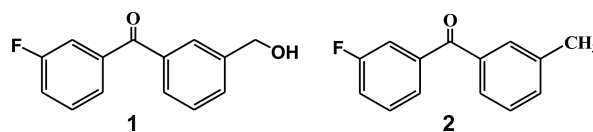


**Figure 1. Chemical structures of 1 and 2.**

questions using results from both DFT computations and time-resolved spectroscopy experiments to probe excited states and intermediates in the photochemistry of interest. Since the reactive intermediates in the *meta* effect photochemical reactions of BP compounds were mainly detected over the nanosecond and microsecond region of time based on our previous studies,<sup>8</sup> we only focused on exploring the competition between the possible photochemical reactions for **1** and **2** using nanosecond TR<sup>3</sup> (ns-TR<sup>3</sup>) and transient absorption (ns-TA) spectroscopy methods. We also compare and contrast the photochemical reactivity found for **1** and **2** with those previously reported for *m*-BPOH,<sup>8b</sup> 3-MeBP,<sup>8d</sup> and 3-FBP.<sup>8e</sup>

## RESULTS AND DISCUSSION

**Will the Photoredox and/or Photosubstitution Reactions Occur in 1?** The preparation of **1** is described in the Experimental Section, and the synthetic route is given in Figure 2S. The ns-TA and ns-TR<sup>3</sup> experimental spectra for **1** were first recorded in CH<sub>3</sub>CN, and these results are presented in Figures 5S and 6S, respectively, in order to characterize its photo-physical processes. These results will be benchmarks to

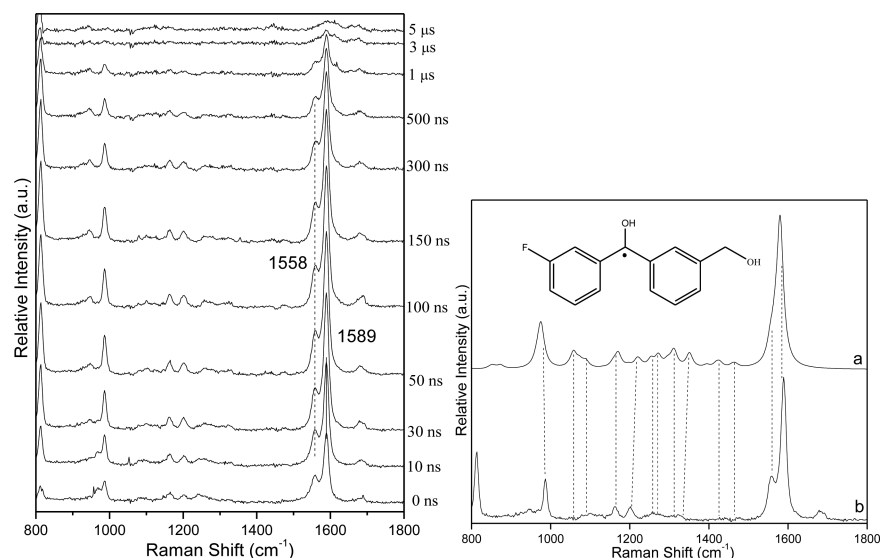


**Figure 2.** Left: ns-TR<sup>3</sup> spectra of **1** in IPA acquired with 266 nm photoexcitation and a 319.9 nm probe wavelength. Right: (a) experimental ns-TR<sup>3</sup> spectrum of **1** taken in IPA at 30 ns with (b) computed normal Raman ketyl radical species with the chemical structure shown above the spectra.

compare to spectra acquired in aqueous media where the photochemical reactions of interest are expected to take place. The ns-TA spectra obtained in CH<sub>3</sub>CN for **1** exhibited the typical electronic absorption bands of the BP triplet excited state at 325 and 525 nm. The triplet excited state of **1** (described as <sup>3</sup>(**1**) subsequently here) has 938, 970, 1170, 1230, 1374, and 1545 cm<sup>-1</sup> resonance Raman bands in its ns-TR<sup>3</sup> spectra, and these vibrational band frequencies agree well with those found in the DFT-calculated normal Raman spectrum of <sup>3</sup>(**1**), as shown in Figure 7S.

The ns-TR<sup>3</sup> spectra of **1** obtained in isopropyl alcohol (IPA) are given in Figure 2. The species with diagnostic Raman bands at 1558 and 1589 cm<sup>-1</sup> was attributed to the ketyl radical intermediate resulting from the hydrogen abstraction reaction between <sup>3</sup>(**1**) and the solvent IPA based on the similarity of these spectra to those reported in ref 9 for the hydrogen abstraction reactions (or photoreduction) of BP with hydrogen donor solvents.<sup>9</sup> Further support for this assignment comes from the good correlation of the vibrational band frequencies for the experimental spectrum to the normal Raman DFT-computed spectrum (Figure 2, right). The photophysical and photochemical processes of **1** in CH<sub>3</sub>CN and IPA look like those of BP and also *m*-BPOH, 3-MeBP, and 3-FBP under analogous solvent conditions.<sup>8b,d,e</sup> This indicates that **1**, which contains two substituents on both *meta* positions, does not induce significant changes on the photophysics and photoreduction of the BP derivatives in nonaqueous solutions, and they behave similarly to the BP parent and the one *meta* position substituent of BP derivatives.

UV-vis spectra were recorded for **1** (10<sup>-5</sup> M, 1:1 H<sub>2</sub>O-CH<sub>3</sub>CN, pH 2, Ar purged) after increasing irradiation time by a low-pressure mercury lamp with its main excitation wavelength at 254 nm. Obviously, an isosbestic point was detected at around 245 nm, suggesting a dynamical photochemical transformation of **1** in acidic aqueous solution. The spectra transformation trend and profile showed great similarity with that of *m*-BPOH under analogous experimental conditions, where the photoredox reaction was detected with the generation of 3-formylbenzhydrol. Therefore, one could expect that the photoredox reaction also takes place for **1**, and the

well-formed UV-vis spectrum in Figure 3 exhibited reasonable similarity with the calculated UV-vis spectrum of 3-fluoro-3'-

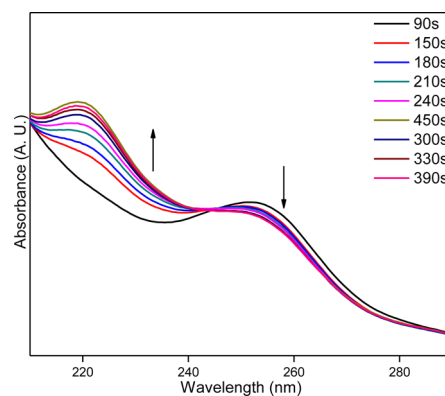


**Figure 3.** UV-vis spectra for **1** in acidic aqueous solutions upon photolysis time, as indicated in the figure.

formylbenzhydrol (Figure 8S). The sample solution (5 × 10<sup>-5</sup> M, 1:1 H<sub>2</sub>O-CH<sub>3</sub>CN, pH 2, Ar purged) after 30 min irradiation was treated as described in the Experimental Section and then analyzed by <sup>1</sup>H NMR and <sup>13</sup>C NMR spectra (Figure 9S). Detection of the benzhydrol proton (δ 5.90 ppm) and the aldehyde proton (δ 9.98 ppm) of 3-fluoro-3'-formylbenzhydrol further supports that the photoredox reaction of **1** takes place in acidic aqueous solutions (Figure 4).

Figure 5 depicts ns-TA spectra of **1** obtained in a pH 0 solution. Compared to the characteristic electronic transient absorption profile of <sup>3</sup>(**1**), the transient species detected in a pH 0 water-containing solution has a shoulder band, and as the

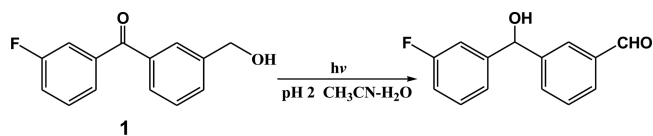


**Figure 4.** Photochemical reaction of **1** in a pH 2 acidic water-containing solution.

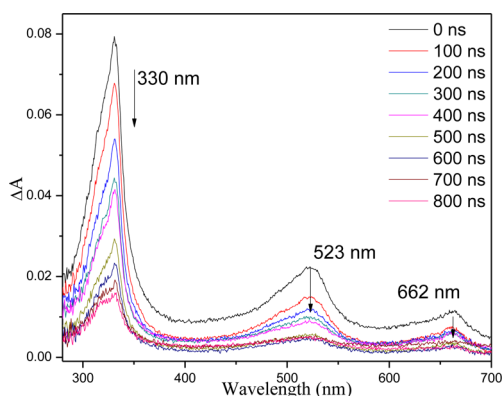


**Figure 5.** Shown are the ns-TA spectra of **1** in a pH 0 solution (1:1, H<sub>2</sub>O/CH<sub>3</sub>CN).

pump and probe delay time increased, the population of the species that contributes to the absorbance at a lower wavelength around 316 nm becomes comparable to the species that absorbs at 330 nm. This change suggests a transformation of <sup>3</sup>(**1**) to a new transient species in a pH 0 acidic water-containing solution. To unravel the photochemical reaction mechanism of **1** in a pH 0 aqueous solution and gain structural information on the species involved, ns-TR<sup>3</sup> experiments were carried out.

The ns-TR<sup>3</sup> spectra (Figure 6) were obtained for **1** in pH 2 and pH 0 CH<sub>3</sub>CN–H<sub>2</sub>O (1:1) solutions using a 266 nm pump

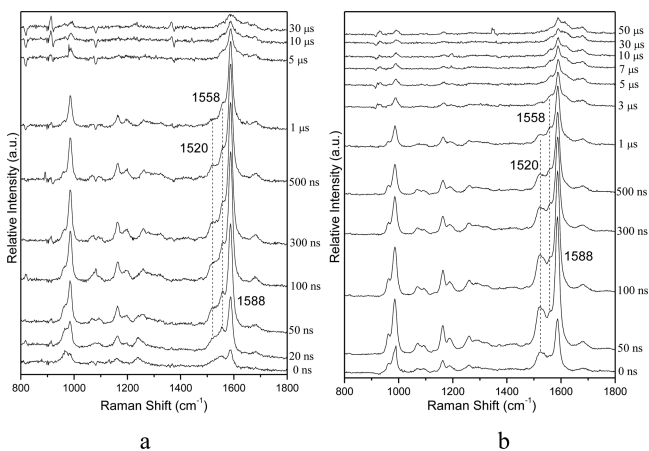


**Figure 6.** ns-TR<sup>3</sup> spectra of **1** in (a) pH 2 solution (1:1, H<sub>2</sub>O/CH<sub>3</sub>CN) and (b) pH 0 solution (1:1, H<sub>2</sub>O/CH<sub>3</sub>CN) acquired with 266 and 319.9 nm pump and probe wavelengths, respectively.

and a 319.9 nm probe. In acidic water-containing solutions, the photohydration, photoredox, and photosubstitution reactions may all possibly take place. We therefore compared the experimental ns-TR<sup>3</sup> spectrum at a delay time of 100 ns recorded in a pH 0 aqueous solution to the computed DFT normal Raman spectrum for the intermediate correlating with the photoredox process and the intermediate associated with the photosubstitution reaction (see Figure 7). The good correlation of the vibrational frequencies for the spectra of Figure 7b,c indicates that the new transient seen in the pH 0 and pH 2 acidic water-containing medium of **1** is the intermediate with its chemical structure above Figure 7b tied to the photoredox reaction. It is noted that biradical species have several resonance structures, and the *meta*-xylylene is the

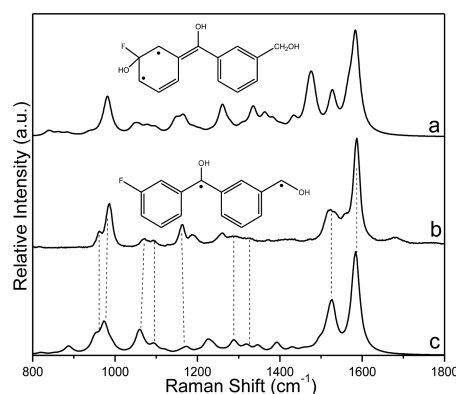


**Figure 7.** (a) Calculated triplet hydration species of **1** at a *meta* position having F (see the chemical structure in the figure) normal in the Raman spectrum. (b) Delay time (50 ns) experimental spectrum taken in a pH 0 CH<sub>3</sub>CN/H<sub>2</sub>O (1:1) solution with  $2.0 \times 10^{-3}$  M of **1**. (c) Biradical species associated with a photoredox reaction of **1** (see the chemical structure in the figure) computed normal in the Raman spectrum.

most stable one.<sup>10</sup> The absence of the strong Raman band around 1480 cm<sup>-1</sup> calculated for the key intermediate associated with the photosubstitution reaction at the *meta* position with F and the photohydration reaction at the *meta* position with a hydroxymethyl group excluded the key intermediate associated with these reactions. Thus, it can be thought that the protonated species of <sup>3</sup>(**1**) containing a positive charge localized at the *meta* site with hydroxymethyl attached is unstable in polar solvents (like in the CH<sub>3</sub>CN–H<sub>2</sub>O solvent system employed here), and this can provide a driver for deprotonation at the *meta*-hydroxymethyl by producing a more stable transient species, such as the biradical species detected in the ns-TR<sup>3</sup> with a diagnostic feature at 1520 cm<sup>-1</sup>. We therefore calculated the electronic absorption spectrum of the biradical species and compared this with the ns-TA spectra of **1** observed in a pH 0 aqueous solution (see Figure 10S). Examination of Figure 10S indicates the new species produced from the protonated species of <sup>3</sup>(**1**) is the biradical species, which is the same one detected in ns-TR<sup>3</sup> experiments. Another transient with a diagnostic Raman band at 1558 cm<sup>-1</sup> emerges after irradiation. Re-examination of the ns-TR<sup>3</sup> spectra for **1** in IPA suggests the band at 1558 cm<sup>-1</sup> probed in acidic aqueous solutions at both pH 2 and pH 0 probably derives some contribution from the ketyl radical species associated with the photoreduction reaction. Detection of ketyl radical transients in water-containing solutions was observed by several groups of researchers over the years.<sup>11–21</sup> In an earlier study by our group, it was suggested that the ketyl radical formation from photoexcitation of BP compounds in aqueous solutions may be formed by a ketone protonation combined with an electron transfer. Hence, the observed 1558 cm<sup>-1</sup> Raman band can be thought to be a characteristic signal for a photoreduction reaction. Both photoredox and photoreduction reactions may provide intensity to the 1588 cm<sup>-1</sup> Raman feature. When the ns-TR<sup>3</sup> experiment was conducted in a pH 2 solution, both reactions may occur and compete with each other. On the other hand, the 1520 cm<sup>-1</sup> band becomes the predominant contribution, and the main photochemical reaction becomes the photoredox reaction in a more acidic condition at pH 0; the 1558 cm<sup>-1</sup> band for the transient of the photoreduction was substantially reduced compared to the 1520 cm<sup>-1</sup> Raman band

attributed to the photoredox process. Compared to *m*-BPOH, the involvement of the electron-withdrawing group F of **1** in the *meta* position makes the carbonyl oxygen group less basic; the photoredox reaction could only be obviously detected under a more acidic condition of pH 0, and the photoreduction reaction is noticeable at pH 2.

The effect of water in such reactions is well-recognized as involving water bridges or water clusters. To simulate the reaction route at an affordable computational time cost, DFT calculations for  $^3(1)$  with two water molecules considered in the calculation system were performed to explore the photoredox reaction pathway at the (U)B3LYP/6-311G\*\* method level, and the energy profile for the photosubstitution and the photoredox reaction are displayed in Figure 8. It is can

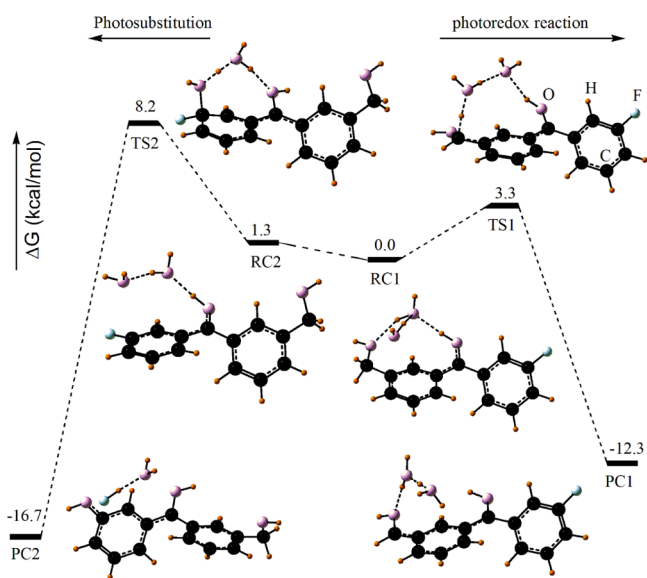
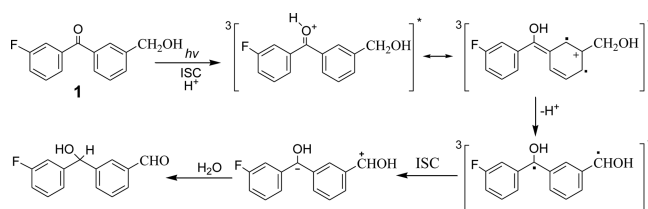


**Figure 8.** Energy profiles for the photosubstitution reaction and the photoredox reaction for **1**.

be reasonably expected that more water molecules will facilitate the reaction by decreasing the reaction barrier. Protonation occurs as the common first step of the photoredox reaction and the photosubstitution reaction for **1**, and this reaction is barrierless for **1** in acidic aqueous media. Subsequent to production of the protonated species, the photosubstitution encounters a 6.9 kcal/mol barrier, while the photoredox process was preferred with a lower 3.3 kcal/mol barrier. The significantly higher energy barrier of the photosubstitution almost excludes the occurrence of the photosubstitution of **1** in aqueous acidic media. These calculation results are consistent with experimental measurements and help explain why the photosubstitution reaction was not detected experimentally for **1** due to competition from the photoredox reaction that has a lower reaction energy. The preceding results were used to develop a probable reaction mechanism for the photoredox process of **1** in aqueous acidic solutions, as depicted in Scheme 5. It is suggested that the *meta* position with F of **1** does not compete with the photoredox process and the photosubstitution was not detected, while the other *meta* position containing the hydroxymethyl moiety is reactive and leads to the overall photoredox reaction observed in the experiments reported here.

**Will the *meta*-Methyl Deprotonation Reaction and/or Photosubstitution Reaction Occur for **2**?** After studying

### Scheme 5. Reaction Mechanism Proposed for the Photoredox of **1** in Acidic Water-Containing Solutions



the photophysics and photochemistry of **1** in several solvents, especially the elucidation of the photoredox reaction in acidic aqueous solutions, we turned to study the photochemical reactions of **2** to determine which photochemical reaction of this compound will occur in acidic aqueous solutions. Time-resolved spectroscopic results for **2** in  $\text{CH}_3\text{CN}$  are given in Figures 11S and 12S. Based on previously reported analyses done for several related BP derivatives, **2** underwent an ISC process in  $\text{CH}_3\text{CN}$ , and no obvious photochemical reaction was observed. The time-resolved spectroscopic results for **2** in pH 7 (see Figure 13S) and pH 2 aqueous solutions (see Figure 14S) exhibited great similarity, and the main photochemical reactions under these conditions were assumed to be the photoreduction reaction based on the similarity of these results to the preceding analysis of **1**.

The photolysis experiment was conducted for **2** ( $10^{-4}$  M, 1:1  $\text{D}_2\text{O}-\text{CH}_3\text{CN}$ , pD 1, Ar purged) for 40 min and analyzed by  $^1\text{H}$  NMR and  $^{13}\text{C}$  NMR spectroscopy (Figure 15S). The detection of the deuterium incorporation to the *m*-methyl group suggests the main photochemical reaction of **2** in acidic  $\text{D}_2\text{O}$ -containing solution was the *meta*-methyl deprotonation, which was the same reaction probed for 3-MeBP as reported. To find information regarding the structure of the transients and unravel the reaction mechanism, ns-TR<sup>3</sup> Raman spectra of **2** were obtained in pH 0 (Figure 9), and the results are obviously different from those observed in the pH 2 and pH 7 water-containing solutions. The main transient with diagnostic

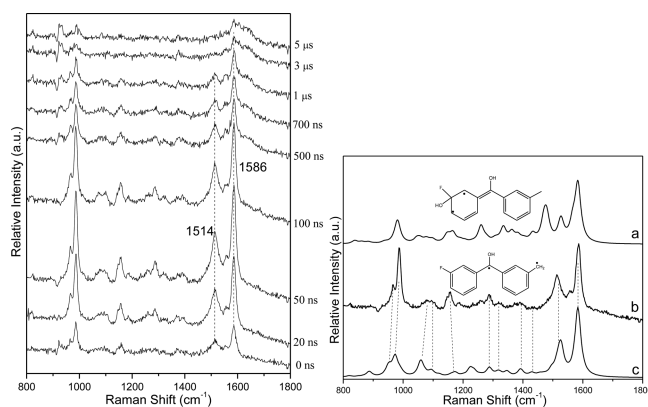


**Figure 9.** (Left) Spectra from ns-TR<sup>3</sup> experiments obtained for **2** in a pH 0 solution (1:1,  $\text{H}_2\text{O}/\text{CH}_3\text{CN}$ ) acquired using 266 nm photolysis and a 319.9 nm probe. (Right) (a) Calculated normal Raman spectrum of the triplet hydration species of **2** (see the chemical structure in the figure) at a *meta* position associated with the photosubstitution reaction. (b) Time delay (50 ns) spectrum acquired in a pH 0  $\text{CH}_3\text{CN}/\text{H}_2\text{O}$  (1:1) solution with  $2.0 \times 10^{-3}$  M of **2**. (c) Normal Raman spectrum computed for the biradical transient (see chemical structure) associated with the *meta*-methyl deprotonation reaction.

bands around 1514 and 1586  $\text{cm}^{-1}$  in Figure 9 exhibits spectra similar to that of the transient observed for the photoredox reaction of **1**, as well as that of the transient species observed for the *meta*-methyl deprotonation reaction for 3-MeBP. Hence, the experimental Raman spectrum of this species recorded at 50 ns was compared with the calculated biradical character intermediate associated with the *meta*-methyl deprotonation reaction of **2**, and the good agreement between these spectra for their vibrational frequency patterns supports the assignment of the main photochemical reaction of **2** under a pH 0 aqueous solution as being attributed to the key biradical character intermediate associated with the *meta*-methyl deprotonation reaction, rather than the photosubstitution that could possibly take place at the *meta* position with the F atom.

DFT calculations for **2** were also conducted using the (U)B3LYP/6-311G\*\* method, and the energy profile of the photosubstitution and the *meta*-methyl deprotonation reaction is displayed in Figure 10. The photosubstitution encounters a

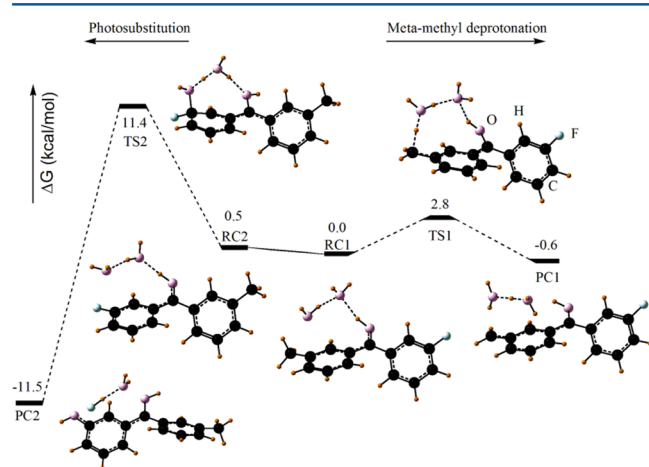
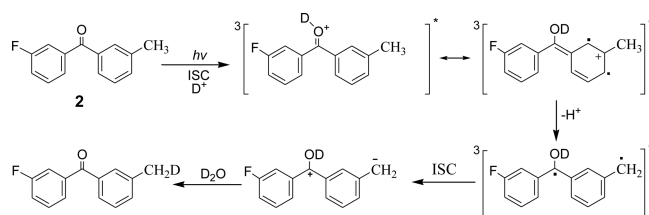


**Figure 10.** Energy profiles for the photosubstitution reaction and the *meta*-methyl deprotonation reaction for **2**.

10.9 kcal/mol barrier, while the *meta*-methyl deprotonation reaction was much preferred due to a lower 2.8 kcal/mol barrier. The significantly higher energy barrier of the photosubstitution almost excludes the occurrence of the photosubstitution reaction of **2** in acidic aqueous solutions. Combining the time-resolved spectroscopic data and results from the DFT computations, the reaction pathway for the *meta*-methyl deprotonation reaction of **2** was proposed and is presented in Scheme 6. Our results in this study indicate that **2** behaves similar to **1** in that the *meta* position with a F atom does not undergo noticeable reaction while the methyl group

#### Scheme 6. Reaction Mechanism Proposed for the *meta*-Methyl Deprotonation of **2** in Acidic Water-Containing Solutions



attached to the other *meta* site undergoes predominant reactions after protonation of the **1** and **2** triplet excited states.

It is noted that the photoredox reaction of **1** was detected in a pH 2 water-containing solution, while the *meta*-methyl deprotonation of **2** was not clearly detected under comparable experimental conditions and was only significant under a more acidic condition in a pH 0 water-containing solution, suggesting the protonation of **1** is easier than that of **2**. This is in accordance with previous studies on *m*-BPOH and 3-MeBP, illustrating that the quantum yield for photoredox of *m*-BPOH ( $\Phi \approx 0.6$ )<sup>7g</sup> is significantly greater than the quantum yield of the *meta*-methyl deprotonation for 3-MeBP ( $\Phi \approx 0.1$ ).<sup>7b</sup> This can likely be explained by the electron-donating OH moiety which stabilizes the biradical intermediate. We also introduced a methoxy moiety to the *meta* site of BP compounds, and the photochemical reactions of 3'-methyl-3-methoxybenzophenone (**3**) and 3'-methoxyl-3-hydroxymethylbenzophenone (**4**) were studied. It is somewhat surprising that no *meta* effect photochemistry was seen for **3** and **4** in acidic water-containing solutions when examined using ns-TR<sup>3</sup> experiments. This is proposed to be caused by the strong electron-donating ability of the methoxy group, which induces the excitation to an  $n\pi^*$  population rather than the  $\pi\pi^*$  transition that leads to the carbonyl oxygen protonation. Additional mechanistic study on these compounds is underway to better understand their very different photochemical behavior.

## CONCLUDING REMARKS

In this study, the photochemical reactions of the BP derivatives **1** and **2** containing two different substituents at the *meta* positions were studied in several different solvent systems using time-resolved spectroscopy experiments and DFT calculations. It was found that **1** can undergo a photoredox reaction and **2** can undergo a *meta*-methyl deprotonation reaction in acidic aqueous solutions.

From examination of results from the present work in conjunction with results from previous studies on *m*-BPOH and 3-FBP, it can be deduced that the introduction of a hydroxyl (or another moiety) that has an electron-donating capacity or of F (or another moiety) that has an electron-withdrawing capacity on the *meta* positions will lead the BP compounds to different photochemical reaction outcomes. On the other hand, when both electron-donating and electron-withdrawing moieties are present, the *meta* positions with the electron-donating moiety were more activated so the BP compounds will undergo the photochemical reaction resulting from this phenyl ring. Thus, the *meta* effect photochemistry could be activated or stifled by changing the substituents on the *meta* positions and changing the pH values of the sample solutions. This new insight into *meta* effect activation of benzophenone derivatives may prove helpful in the design and development of photoremovable protecting groups based on *meta*-substituted benzophenone derivatives such as KP derivatives and other systems.

## EXPERIMENTAL SECTION

**Synthesis of Compound 1 and Photolysis Experiment.** 3-Fluoro-3'-methylbenzophenone (compound **2**) was commercially available (CAS: 864087-22-9), and its <sup>1</sup>H NMR spectrum is given in Figure 1S in the Supporting Information. 3-Hydroxymethyl-3'-fluorobenzophenone (compound **1**) was synthesized from compound **2** following a similar reaction route of *m*-BPOH as reported in ref 7c, and a brief description is presented in the Supporting Information

along with the  $^1\text{H}$  NMR spectra, which estimated the purity of **1** to be greater than 98% (Figure 3S). The  $^{13}\text{C}$  NMR spectrum of **1** is provided in Figure 4S.

The sample solution of  $5 \times 10^{-5}$  M was purged with Ar for 15 min and was irradiated with two 254 nm lamps for 2 min of photolysis.  $\text{CH}_2\text{Cl}_2$  was used for extraction of the photolyzed mixture twice, and the  $\text{CH}_2\text{Cl}_2$  layer was dried with anhydrous  $\text{MgSO}_4$ . This was filtered, and the solvent was taken away in vacuo and characterized via  $^1\text{H}$  NMR ( $\text{CDCl}_3$ ).

**ns-TA and ns-TR<sup>3</sup> Experiments and DFT Computations.** The ns-TA and ns-TR<sup>3</sup> experiments and methods have been previously given, and one is referred to refs 8c and 8d for the experimental details. Similarly, the description of the DFT calculations, including the method, basis sets, and software (e.g., (U)B3LYP/6-311G\*\* and Gaussian 03) used was previously reported, and the reader is referred to ref 8d for details and the Supporting Information for selected results from the calculations discussed in this article.

## ■ ASSOCIATED CONTENT

### ■ Supporting Information

The Supporting Information is available free of charge on the ACS Publications website at DOI: 10.1021/acs.joc.6b00698.

UV-vis absorption spectra and NMR spectra for reactant and photoproduct species discussed in the text; fs-TA and ns-TR<sup>3</sup> spectra for some of the excited states and intermediate species discussed in the text; UB3LYP/6-311G\*\* computed RC, TS, and PC optimized geometries and the reaction energy pathway as well as TD-DFT (UB3LYP/6-311G\*\*) oscillator strength and excited state energies for selected intermediates; (U)B3LYP/6-311G\*\* computed optimized geometry Cartesian coordinates, total energies, and vibrational zero-point energies for the species discussed in the text (PDF)

## ■ AUTHOR INFORMATION

### ■ Corresponding Authors

\*E-mail: anini1984@163.com.

\*E-mail: phillips@hku.hk.

### ■ Notes

The authors declare no competing financial interest.

## ■ ACKNOWLEDGMENTS

This work was financed in part by the Research Grants Council of Hong Kong (Grant HKU 17301815) to D.L.P., the Areas of Excellence Scheme (AoE/P-03/08) and the Special Equipment Grant (SEG HKU/07). J.M. thanks the National Science Fund (21503167), Shaanxi Province Science Fund (2016JQ2009), and Northwest University (338020011, 2016129) for support of this project.

## ■ REFERENCES

- (1) Golan, A.; Bravaya, K. B.; Kudirka, R.; Kostko, O.; Leone, S. R.; Krylov, A. I.; Ahmed, M. *Nat. Chem.* **2012**, *4*, 323–329.
- (2) Klan, P.; Wirz, J. *Photochemistry of Organic Compounds: From Concepts to Practice*; Wiley: Hoboken, NJ, 2009; ISBN: 9781444300017.
- (3) Ramseier, M.; Senn, P.; Wirz, J. *J. Phys. Chem. A* **2003**, *107*, 3305–3315.
- (4) (a) Zimmerman, H. E. *J. Am. Chem. Soc.* **1995**, *117*, 8988–8991. (b) Zimmerman, H. E. *J. Phys. Chem. A* **1998**, *102*, 5616–5621.
- (5) (a) Bosca, F.; Marin, M. L.; Miranda, M. A. *Photochem. Photobiol.* **2001**, *74*, 637–655. (b) Castell, J. V.; Gomezlechón, M. J.; Miranda, M. A.; Morera, I. M. *J. Photochem. Photobiol., B* **1992**, *13*, 71–81.

- (c) Encinas, S.; Miranda, M. A.; Marconi, G.; Monti, S. *Photochem. Photobiol.* **1998**, *68*, 633–639. (d) Jimenez, M. C.; Miranda, M. A.; Tormos, R.; Vaya, I. *Photochem. Photobiol. Sci.* **2004**, *3*, 1038–1041. (e) Bosca, F.; Miranda, M. A.; Carganico, G.; Mauleon, D. *Photochem. Photobiol.* **1994**, *60*, 96–101. (f) Bosca, F.; Miranda, M. A. *J. Photochem. Photobiol., B* **1998**, *43*, 1–26.
- (6) (a) Martinez, L. J.; Scaiano, J. C. *J. Am. Chem. Soc.* **1997**, *119*, 11066–11070. (b) Cosa, G.; Martinez, L. J.; Scaiano, J. C. *Phys. Chem. Chem. Phys.* **1999**, *1*, 3533–3537. (c) Vinette, A. L.; McNamee, J. P.; Bellier, P. V.; McLean, J. R. N.; Scaiano, J. C. *Photochem. Photobiol.* **2003**, *77*, 390–396. (d) Llauger, L.; Cosa, G.; Scaiano, J. C. *J. Am. Chem. Soc.* **2002**, *124*, 15308–15312. (e) Llauger, L.; Miranda, M. A.; Cosa, G.; Scaiano, J. C. *J. Org. Chem.* **2004**, *69*, 7066–7071. (f) Lukeman, M.; Scaiano, J. C. *J. Am. Chem. Soc.* **2005**, *127*, 7698–7699.
- (7) (a) Lukeman, M.; Xu, M.; Wan, P. *Chem. Commun.* **2002**, *2*, 136–137. (b) Huck, L. A.; Wan, P. *Org. Lett.* **2004**, *6*, 1797–1799. (c) Mitchell, D.; Lukeman, M.; Lehnerr, D.; Wan, P. *Org. Lett.* **2005**, *7*, 3387–3389. (d) Basarić, N.; Mitchell, D.; Wan, P. *Can. J. Chem.* **2007**, *85*, 561–571. (e) Hou, Y.; Wan, P. *Photochem. Photobiol. Sci.* **2008**, *7*, 588–596. (f) Hou, Y.; Huck, L. A.; Wan, P. *Photochem. Photobiol. Sci.* **2009**, *8*, 1408–1451. (g) Mitchell, D. P. *The intramolecular photoredox behaviour of substituted benzophenones and related compounds*. Ph.D Thesis, University of Victoria, 2008.
- (8) (a) Chuang, Y. P.; Xue, J. D.; Du, Y.; Li, M. D.; An, H. Y.; Phillips, D. L. *J. Phys. Chem. B* **2009**, *113*, 10530–10539. (b) Ma, J.; Li, M.-D.; Wan, P.; Phillips, D. L. *J. Org. Chem.* **2011**, *76*, 3710–3719. (c) Ma, J.; Su, T.; Li, M. D.; Du, W.; Huang, J.; Guan, X.; Phillips, D. L. *J. Am. Chem. Soc.* **2012**, *134*, 14858–14868. (d) Ma, J.; Su, T.; Li, M.-D.; Zhang, X.; Huang, J.; Phillips, D. L. *J. Org. Chem.* **2013**, *78*, 4867–4878. (e) Huang, J.; Ma, J.; Li, M.; Liu, M.; Zhang, X.; Phillips, D. L. *J. Org. Chem.* **2015**, *80*, 9425–9436.
- (9) Kavarnos, G. J.; Turro, N. J. *Chem. Rev.* **1986**, *86*, 401–449.
- (10) (a) Hammad, L. A.; Wenthold, P. G. *J. Am. Chem. Soc.* **2000**, *122*, 11203–11211. (b) Neuhaus, P.; Grote, D.; Sander, W. *J. Am. Chem. Soc.* **2008**, *130*, 2993–3000.
- (11) Ledger, M. B.; Porter, G. *J. Chem. Soc., Faraday Trans. 1* **1972**, *68*, 539–553.
- (12) Ireland, J. F.; Wyatt, P. A. H. *J. Chem. Soc., Faraday Trans. 1* **1973**, *69*, 161–168.
- (13) Rayner, D. M.; Wyatt, P. A. H. *J. Chem. Soc., Faraday Trans. 2* **1974**, *70*, 945–954.
- (14) Favaro, G.; Bufalini, G. *J. Phys. Chem.* **1976**, *80*, 800–804.
- (15) Rayner, D. M.; Tolg, P. K.; Szabo, A. G. *J. Phys. Chem.* **1978**, *82*, 86–89.
- (16) Shizuka, H.; Kimura, E. *Can. J. Chem.* **1984**, *62*, 2041–2046.
- (17) Bensasson, R. V.; Gramain, J. C. *J. Chem. Soc., Faraday Trans. 1* **1980**, *76*, 1801–1810.
- (18) Lounnot, D. J.; Jacques, P.; Fouassier, J. P.; Casal, H. L.; Kim Thuan, N.; Scaiano, J. C. *Can. J. Chem.* **1985**, *63*, 3001–3006.
- (19) Hoshi, M.; Shizuka, H. *Bull. Chem. Soc. Jpn.* **1986**, *59*, 2711–2715.
- (20) Elisei, F.; Favaro, G.; Gerner, H. *J. Photochem. Photobiol., A* **1991**, *59*, 243–253.
- (21) Canonica, S.; Hellrung, B.; Wirz, J. *J. Phys. Chem. A* **2000**, *104*, 1226–1232.